JOURNAL OF SOLID STATE CHEMISTRY 39, 75–84 (1981)

Valence State of the Fe Ions in $Sr_{1-y}La_yFeO_3$

M. TAKANO,* J. KAWACHI, N. NAKANISHI AND Y. TAKEDA†

Department of Chemistry, Faculty of Science, Konan University, Kobe, 658, Japan, and † Department of Chemistry, Faculty of Engineering, Mie University, Tsu, 514, Japan

Received December 11, 1980

The $Sr^{2+}_{1-y}La^{3+}_yFeO_3$ system with $0.1 \leqq y \leqq 0.6$ has been studied mainly by the Mössbauer effect. The results are discussed referring to the $Ca_{1-x}Sr_xFeO_3$ system. The following four kinds of electronic phases have been observed: the paramagnetic and the antiferromagnetic average valence phases and the corresponding mixed valence phases. Two kinds of Fe ions coexist, in general, in the mixed valence phases. In the antiferromagnetic mixed valence phase, typically at 4 K, the magnetic hyperfine field and the center shift each takes a wide range of value depending on the composition, while a beautiful correlation is kept between them. The extreme values are close to those expected for Fe^{3+} and Fe^{5+}. The appropriate chemical formulas are, therefore, $Ca_{1-x}Sr_xFe^{(3+\Delta)+}_{0.5}Fe^{(5-\Delta)+}_{0.5}O_3$ and $Sr_{1-y}La_yFe^{(3+\delta)+}_{(1+y)/2}Fe^{(5-\delta)+}_{(1-y)/2}O_3$.

Introduction

Preparations and characterizations of oxides containing appreciable quantities of iron in a rare valence state +4 have been reported by several research groups. All of these oxides have the perovskite-type or some related structures stabilized by the presence of large alkaline earth cations.

The ideal perovskite formula is $AFe^{4+}O_3$ (A: Ca, Sr, and Ba). The stoichiometric phase of $SrFeO_3$ was successfully prepared under high oxygen pressures of 33–87 MPa by MacChesney *et al.* (*1*). This oxide has been characterized by the cubic structure, a temperature-independent electrical resistivity of $\approx 10^{-2}$ ohm cm and an antiferromagnetic screw spin structure (T_N = 134 K, 3.1 μ_B/Fe at 4 K) (*1, 2*). The Mössbauer effect (ME) was applied by Gallagher *et al.* (*3*), and the center shift (CS) at room temperature of 0.05 mm/sec and the magnetic hyperfine field (Hi) at 4 K of 33.1 T have, thereafter, been referred to as the typical values for Fe^{4+}.

The preparation and the characterization of $CaFeO_3$ were reported and discussed in our recent papers (*4, 5*). The oxygen pressure applied was 2 GPa. The structure is slightly distorted from cubic symmetry and a change in temperature dependence of electrical resistivity occurs at about 116 K, where magnetic susceptibility reaches its antiferromagnetic peak. The ME spectrum at room temperature is very similar to that of $SrFeO_3$, but, at 4 K, two sets of magnetic splittings with the same intensities but with greatly different CS's and Hi's are seen. Moreover,

* Author to whom correspondence should be addressed.

0022-4596/81/100075-10$02.00/0

the averaged CS and Hi values are very close to the corresponding parameters of $SrFeO_3$ at 4 K. The sharp contrast between these two stoichiometric oxides at 4 K has been explained by assuming a charge disproportionation into equal numbers of Fe^{3+} and "Fe^{5+}" in $CaFeO_3$ (*5*); i.e., $2Fe^{4+}$ $(t^3\sigma^{*1}) \rightarrow Fe^{3+}$ (t^3e^2) + Fe^{5+} (t^3). This idea has been proposed to be applicable also to the cases of slightly oxygen deficient phases such as $Sr_3Fe_2O_{6.9}$ and $BaFeO_{2.95}$, each exhibiting at 4 K a spectrum similar to that of $CaFeO_3$. It should be noted here that $SrFeO_3$ is the unique exceptional oxide showing a single-component spectrum at 4 K.

This model was very challenging because Fe^{5+} was quite a rare valence state at that time, that had been detected only as a dilute impurity in $SrTiO_3$ by ESR (*6*). And this was a simple model because classification of ions by nominal valences is generally a mere starting point of an understanding of the real electronic states. Moreover, the mechanism to bring about the disproportionation has not been clear. Thus, for a further examination and refinement of our model experimental works on various series of oxides have been made. The results for $Ca_{1-x}Sr_xFeO_3$ $(0 \leqq x \leqq 1)$ (*7*), $Sr_{1-y}La_yFeO_3$ $(y = 0.5)$ (*8*), and $SrFeO_{3-z}$ (*9*) were partly reported already. In this paper measurements of powder X-ray diffraction, magnetization, and the ME on the solid solutions of $SrFeO_3$ and $LaFe^{3+}O_3$, $Sr_{1-y}La_yFeO_3$ $(0.1 \leqq y \leqq 0.6)$ will be described in detail.

Shimoney and Knudsen (*10*) and Gallagher and MacChesney (*11*) (this work will be referred to as GM, hereafter) reported the ME of this system. A composition-dependent average valence state due to a rapid electron exchange between the Fe ions was observed for each phase with $y \leqq 0.6$ at room temperature. GM interpreted the complex spectra at lower temperatures as indicating the resolution into the individual valence states, Fe^{3+} and Fe^{4+}, and discussed possible mechanisms. However, we can point out some basic difficulties in their interpretation, which are similar to those discussed in Ref. (*5*). For example, though $Fe^{3+}/Fe^{4+} = 4/6$ for $Sr_{0.6}La_{0.4}FeO_3$, the intensity ratio of the corresponding components was indicative of $Fe^{3+}/Fe^{4+} > 1$. So, expecting the applicability of our model to this series of oxides or such an electron localization as producing Fe^{3+} and Fe^{5+}, we have obtained the ME data over a wide composition range at various temperatures.

Experimental

(i) Sample Preparation

Compositions x = 0.1, 0.2, 0.3, 0.5, and 0.6 were prepared as follows. Well dried raw materials, $SrCO_3$, La_2O_3, Fe_2O_3, each with a purity of 99.9% were weighed and were mixed thoroughly in an agate mortor. The mixtures were heated on platinum sheets at 1273 K for 20 hr. After grinding and mixing, the subsequent treatment at about 1470 K for 24 hr was carried out. This process was repeated three times in an effort to attain thorough homogeneity. Then, each product was divided into several portions, and these were annealed under various conditions to increase the oxygen content. Oxygen pressures of 100–150 MPa were applied at 673–873 K for 170–500 hr by the method described in Ref. (*12*).

(ii) Measurements

X-Ray diffraction on powdered samples was made using Ni-filtered Cu$K\alpha$ radiation in a range $5° \leqq 2\theta \leqq 100°$. Cell dimensions were calculated from high-angle reflections obtained by scanning at 1°/8

min. Silicon of 99.999% was employed as the standard material.

Magnetization was measured by the Faraday method in a temperature range from room temperature to 77 K.

Electrical resistivity of sintered bodies was measured by the usual four-terminal method in the same temperature range as that for magnetization.

The ME of ^{57}Fe was performed at various temperatures between room temperature and 77 K and at 4 K using a $^{57}Co(Cu)$ source kept at room temperature. The velocity was calibrated by using pure iron metal as the standard material.

Results and Discussion

(i) X-Ray Diffraction

The main purpose of this study is to investigate the electronic state of the Fe ions by measuring the dependence of the ME on the La content. By the way, it is known that the introduction of oxygen vacancies into $SrFeO_3$ can give rise to a substantial change in the electronic state as clearly seen in the ME spectrum of $SrFeO_{2.86}$ (*3, 5, 9*). So, samples prepared under various oxygen pressures have been tested for the purpose of making it certain by comparison that the ME results to be reported in this paper are free from nonstoichiometric effects.

GM reported to have successfully obtained the stoichiometric phases with $0.2 \leqq y \leqq 0.8$ by annealing under oxygen pressures of about 10^2 MPa at 891 K for 170 hr. According to their X-ray diffraction analysis, the introduction of La within $y \leqq 0.4$ simply enlarges the cubic unit cell, while a distortion is induced when $y \geqq 0.5$. This is rhombohedral for $y = 0.5$, 0.6 and orthorhombic for $y = 0.8$.

The results of our measurements can be summarized briefly as follows. (a) For any composition, the diffraction pattern is independent within experimental error upon the annealing conditions we used, and the cell dimensions are in excellent agreement with those given by GM. These facts strongly suggest the ideal oxygen contents in our annealed samples, because these were generally treated under higher oxygen pressures for longer times than GM's. The typical samples to appear in this paper are listed in Table I. (b) The diffraction pattern of sample (C) can be explained better by taking a slight rhombohedral distortion into account, though GM assigned cubic structure to compositions $y \leqq 0.4$. (c) The use of high oxygen pressures becomes less important with the increasing La content. For example, a sample with $y = 0.1$ quenched from 1490 K in the air is considerably oxygen deficient and shows a distortion from cubic symmetry and a remarkable increase in cell volume at the same time. However, such changes cannot be detected for $y = 0.6$.

These results are completely consistent with the other measurements. Mentioning an example for simplicity, the air-quenched sample with $y = 0.1$ shows paramagnetic behavior at 77 K because of a great reduction in the antiferromagnetic transition temperature due to oxygen deficiency, while there are little or no such effects for $y = 0.3$–0.6.

(ii) The Mössbauer Effect and Other Measurements

In this section microscopic information obtained by the ME will be presented and discussed referring to macroscopic magnetic and electrical properties.

(ii.1) Magnetic and Electrical Properties

For measurements of magnetization samples were initially cooled to 77 K with or without an applied field of 0.64 MA/m and then heated slowly ($\approx$1

TABLE I

$Sr_{1-y}La_yFeO_3$ SAMPLES

Sample	Composition y	Final heat treatment			Cell dimensions		T_m (K)[a]
		p_{O_2} (MPa)	Temp. (K)	Time (hr)	Present work	GM	
A	0.1	130	873	170	cubic a = 0.38590 nm	y = 0 cubic a = 0.3850 nm	114
B	0.2	150	873	170	cubic a = 0.38652 nm	y = 0.2 cubic a = 0.3865 nm	139
C	0.3	130	873	456	rhombohedral a = 0.3873 nm α = 90.05	y = 0.4 cubic a = 0.3880 nm	199
D	0.5	130	873	500	—[b]	rhombohedral a = 0.3889 nm α = 90.26°	230
E	0.6	110	673	170	—[b]	rhombohedral a = 0.3896 nm α = 90.333°	>300

[a] The temperature of a magnetic anomaly (see Fig. 1).
[b] The data given by GM explain very well the diffraction pattern of the present sample.

K/min) up to room temperature in a fixed field of 0.422 MA/m. The results for the field-cooled samples are shown in Fig. 1. Residual magnetization was found for samples (C) (only when field cooled), (D) and (E) at 77 K, and only for sample (E) at room temperature. The values at 77 K are 7×10^{-4} μ_B/Fe, 6.4×10^{-3} μ_B/Fe, and 7.34×10^{-2} μ_B/Fe for (C), (D), and (E), respectively. Samples (A)–(E) thus seem to be antiferromagnets accompanied with or without parasiticferromagnetism depending on crystalline distortion from cubic symmetry.

Figure 2 shows the temperature dependence of electrical resistivity of samples (C) and (D). For each semiconductor, an intermediate region beginning in the vicinity of the magnetically anomalous temperature (T_m, see Fig. 1) is sandwiched between the regions where log ρ depends linearly on $1/T$. On the other hand, partly stating the results in advance, the ME in the intermediate region revealed

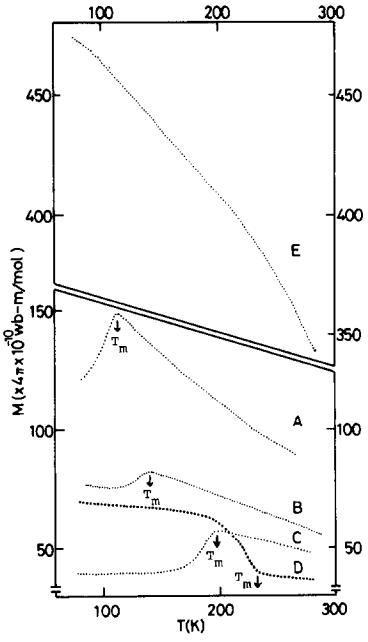

FIG. 1. Temperature dependence of magnetization (field cooled).

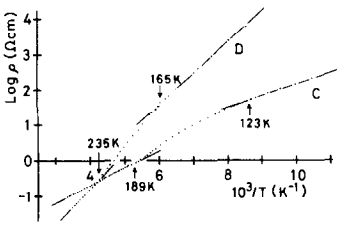

FIG. 2. Temperature dependence of electrical resistivity of samples (C) and (D).

an unusual coexistence of the paramagnetic and the antiferromagnetic portions. Thus, the magnetic anomalies of samples (A)–(E) indicate, at least, the occurrence of the antiferromagnetically ordered portions in the crystals below the T_m's.

(ii.2) The Mössbauer Effect

The typical spectra at room temperature and 4 K are shown in Figs. 3 and 4, respectively. As for the spectra at room temperature it would be most interesting to test the idea of average valence state. The criterion employed by the previous investigators would have been whether the spectrum of a given composition consisted of two components with an intensity ratio proper to the composition at ≈0.05 mm/sec (the CS of $SrFeO_3$) and

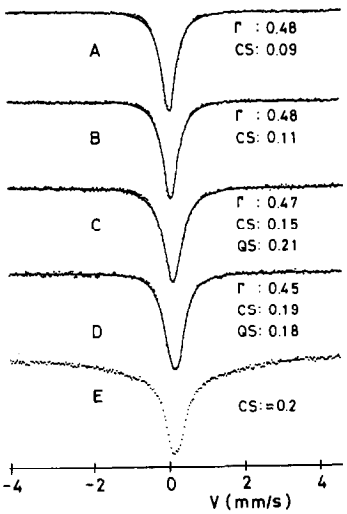

FIG. 3. Mössbauer spectra at room temperature.

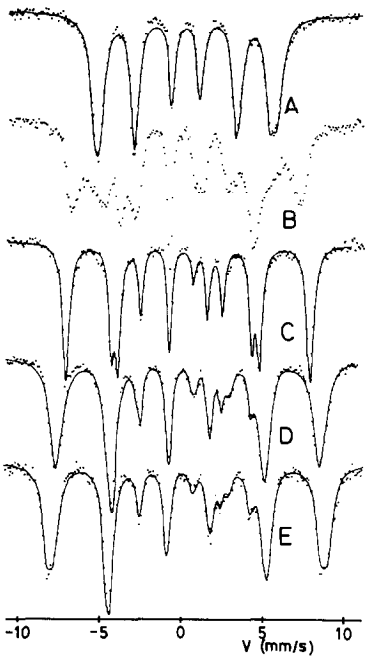

FIG. 4. Mössbauer spectra at 4 K.

≈0.39 mm/sec (the CS of $LaFeO_3$ (*13*)), or of a unique component having an intermediate CS. As can be seen in Fig. 3, the latter is the case for any composition beyond doubt.

The line shape is, however, not perfectly symmetric for any composition, because the absorption is intensified slightly on the positive velocity side. And the linewidth is about twice as large as that for metallic iron even for the cubic phases. A precise analysis would require a distribution in CS and would reveal an interesting dependence of CS upon the local La content. However, such an analysis is not very important for our purpose at the present stage, and shown in Fig. 3 by the solid lines are the simplest and satisfactory computer fittings obtained by assuming a single Lorentzian line for each cubic phase and a pair of Lorentzian lines with the same intensities and the same widths for each rhombohedral phase. The doublets for the rhombohedral phases have been assumed to be due to

quadrupole interactions. The parameter values are given in Fig. 3. The spectrum for $y = 0.6$ has a magnetically perturbed background, which is consistent with the magnetic measurement indicating a T_m above 300 K. As shown in Fig. 5 the CS depends on the composition linearly. Thus, any remarkable evidence against the idea of average valence state has not been found.

GM stated to have observed the resolution into the distinct valence states, Fe^{3+} and Fe^{4+}, at low temperatures. Indeed, two or more components can be seen in each spectrum at 4 K. However, it is readily noted, firstly, that the CS and the Hi are not fixed but depend largely on the composition. Secondly, the intensity ratio is far from those expected from the formula $Sr_{1-y}La_yFe^{3+}_yFe^{4+}_{1-y}O_3$, as briefly discussed in a previous section. The analysis of these spectra and the comparison of the derived parameters with those for $Ca_{1-x}Sr_xFeO_3$ to be described below have led us to assign the formulas, $Ca_{1-x}Sr_xFe^{(3+\Delta)+}_{0.5}Fe^{(5-\Delta)+}_{0.5}O_3$ and $Sr_{1-y}La_yFe^{(3+\delta)+}_{(1+y)/2}Fe^{(5-\delta)+}_{(1-y)/2}O_3$, to these oxides.

The most typical resolution has been manifested by sample (C). The spectrum can be fitted quite satisfactorily by using two sets of magnetic hyperfine patterns. For each component the usual intensity ratio for a powder pattern of 3:2:1:1:2:3 and, as for the linewidth (Γ), Γ(line 1) = $\Gamma(6)$, $\Gamma(2) = \Gamma(5)$, and $\Gamma(3) = \Gamma(4)$ are assumed, where the lines are numbered from the left-hand side. The latter assumption is made to take slight distributions in the parameters into account conveniently. The best parameters sought by changing the line widths stepwise are given in Table II. The relative intensity of the two components, 66:34, is in excellent agreement with the ratio $(1 + y)/2:(1 - y)/2 = 65:35$. The small quadrupole interaction found at room temperature seems to be disguised at 4 K. This might be due to a complex spin structure resulting in varied orientations of the Hi's relative to the electric field gradient axes.

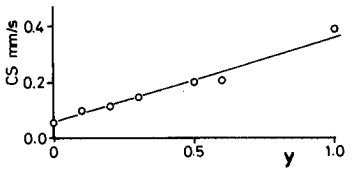

FIG. 5. Composition dependence of the CS at room temperature.

When the La content is decreased, the resolution becomes poor, and the spectrum for $y = 0.1$ looks like a broadened single magnetic pattern. However, the lines on the positive velocity side are broader than the corresponding ones on the negative velocity side (Γ (1) < $\Gamma(6)$ etc.), and this suggests that the spectrum can be resolved into components for which a more positive CS is invariably accompanied with a larger Hi. The calculated solid-line spectrum in Fig. 4 consists of two magnetic patterns with a relative intensity close to the expected value. The patterns are subject to the same constraints as those for sample (C).

The spectrum of sample (B) shows an enhanced resolution. In comparison with the spectrum of sample (C) the outer lines are considerably broader, and a less intense pattern of sample (A)-type seems to be superimposed additionally though X-ray diffraction ruled out any phase separation. These indicate that the electronic state of the Fe ions varies significantly with the locally fluctuating La content around $y = 0.2$. The relative intensity of the two main components seems to be not far from $(1 + y)/2:(1 - y)/2 = 60:40$.

The composition $y = 0.4$ studied by GM showed a very clearcut resolution into a pair of components similarly to sample (C). The intensity ratio is favorable to our model.

On the other hand, both samples (D)

TABLE II

MÖSSBAUER DATA (4 K)

Sample	Component	CS (mm/sec)	Hi (T)	I (%)	Linewidth (mm/sec) Γ(1)	Γ(2)	Γ(3)
	I	0.20	34.5	56	0.71	0.62	0.44
A	II	0.12	32.8	44	0.62	0.53	0.44
	av	0.16	33.6				
	I	~0.33	~43	~60			
B	II	~0.05	~31	~40			
	av	~0.19	~37				
	I	0.36	46.0	66	0.52	0.42	0.34
C	II	−0.05	26.9	34	0.38	0.36	0.33
	av	0.16	36.5				
	I	0.44	50.5	72	0.94	0.67	0.46
D	II	0.00	26.2	13	0.46	0.35	0.31
	II′	0.10	29.8	15	0.58	0.51	0.33
	av	0.25	39.3				
	I	0.44	54.2	39	0.71	0.53	0.36
	I′	0.42	50.4	37	0.71	0.53	0.36
E	II	−0.05	26.6	14	0.53	0.44	0.36
	II′	0.12	29.3	10	0.53	0.44	0.36
	av	0.23	40.1				

and (E) show more complicated spectra in each of which absorption lines from three different components can be readily pointed out. These spectra have been analyzed tentatively by using unusually broad widths for the outer lines to obtain approximate parameter values. The calculated spectrum for sample (D) consists of three components and that for sample (E) does of four components. Though the presence of more than two kinds of components is beyond our model, we suggest that these can be divided into two groups according to the great differences in CS and Hi and that the relative intensity is close to the expected value as seen in Table II.

The CS's and the Hi's obtained above are plotted in Fig. 6 together with the data for $Ca_{1-x}Sr_xFeO_3$. As described in Ref. (*7*) the spectra of this series of oxides at 4 K also show the coexistence of equal amounts of Fe ions in two different charge states. The differences in CS and Hi lessen with the increasing Sr content to disappear at $x = 1$. Figure 6a shows the values for each component and Fig. 6b shows the averaged values corresponding to the virtual Fe^{4+} state. It is quite noticeable in Fig. 6a that the CS and the Hi each takes a wide range of value keeping a beautiful correlation between them. The averaged values show a good convergence around the point with CS = 0.15 mm/sec and Hi = 33 T, which are close to the parameters for $SrFeO_3$. The significant deviation to the upper right and the presence of more than two kinds of Fe ions in

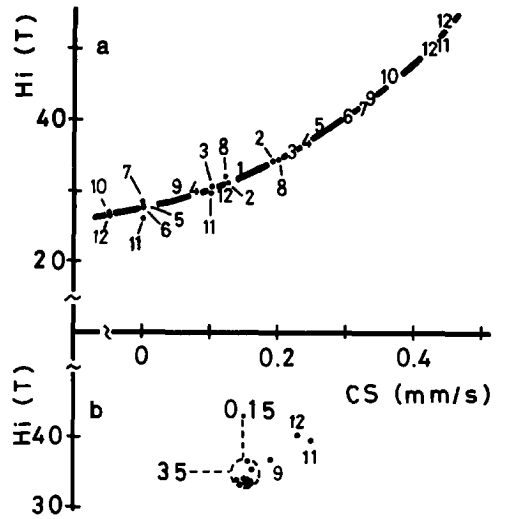

$Ca_{1-x}Sr_xFeO_3$, 1 : x = 1, 2 : x = 0.75, 3 : x = 0.625, 4 : x = 0.5, 5 : x = 0.25, 6 : x = 0.125, 7 : x = 0.

$Sr_{1-y}La_yFeO_3$, 8 : y = 0.1, 9 : y = 0.2, 10 : y = 0.3, 11 : y = 0.5, 12 : y = 0.6.

FIG. 6. Mössbauer data for $Ca_{1-x}Sr_xFeO_3$ and $Sr_{1-y}La_yFeO_3$. (a) Data for different valence states, and (b) data for the virtual Fe^{4+} state.

$Sr_{0.5}La_{0.5}FeO_3$ and $Sr_{0.4}La_{0.6}FeO_3$ may suggest some qualitative change in chemical bonding.

Müller *et al.* (*6*) reported the resonance parameters of $g = 2.0131$ and $A(^{57}Fe) = 8.6 \pm 0.1$ cm^{-1} (Hi = 28 ± 0.3 T) for Fe^{5+} in $SrTiO_3$. And our very recent ME measurement on $SrTiO_3$ codoped with ^{57}Fe and Al (Ti:^{57}Fe:Al = 994:1:5) (*14*) indicated a CS of 0.00 ± 0.03 mm/sec for Fe^{5+} at 4 K. These values are very close to those for, for example, $CaFeO_3$ and $Sr_{0.7}La_{0.3}FeO_3$. On the other hand, the typical values for Fe^{3+} in orthoferrites are CS ≈ 0.5 mm/sec and Hi ≈ 55 T, which are close to those for $Sr_{0.5}La_{0.5}FeO_3$ and $Sr_{0.4}La_{0.6}FeO_3$. Figure 6a thus indicates that the Fe ions can take indiscrete states between Fe^{3+} and Fe^{5+} depending on the composition. So, by recognizing Fe^{3+} and Fe^{5+} as the ideal localized (ionic) states and Fe^{4+} as the ideal delocalized state, we can apply the following simplified chemical formulas to the mixed valence phases of these oxides; $Ca_{1-x}Sr_xFe_{0.5}^{(3+\Delta)+}Fe_{0.5}^{(5-\Delta)+}O_3$ and $Sr_{1-y}La_y Fe_{(1+y)/2}^{(3+\delta)+}Fe_{(1-y)/2}^{(5-\delta)+}O_3$, where both Δ and δ increase up to unity as the Sr content increases.

Measurements around the T_m's were made on samples (C), (D) and also on $SrFeO_3$ (this sample was kindly supplied by Professor M. Shimada, Osaka University) to observe the valence change, especially in relation to the magnetic transition. Figure 7 shows the spectra of sample (C). It is noticeable that the paramagnetic and the antiferromagnetic patterns are superimposed over a wide temperature range. The resolution into the different valence states can be clearly seen in the double magnetic patterns, while not in the paramagnetic one. The lineshape of the magnetic patterns is sharp enough to rule out such a wide distribution in the Néel temperature (T_N) and the intensity is weakened to vanish asymptotically near the T_m. Sample (D) behaves similarly in general, while a considerable reduction in the Hi's can be fol-

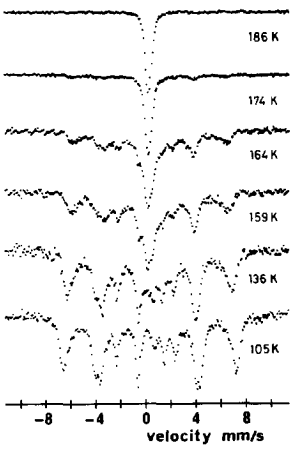

FIG. 7. Temperature dependence of the Mössbauer spectrum of sample (C).

lowed as the T_m is approached. The room temperature spectrum of sample (E) (Fig. 3) also suggests common behavior.

We interpret these results as indicating the coexistence of the paramagnetic average valence phase and the antiferromagnetic mixed valence phase (these will be abbreviated to *Pa* and *Am*, respectively), the domains in the former phase successively making a first-order transition to the latter phase below the T_m. The T_N of the mixed valence phase seems to coincide with the T_m at least for samples (D) and (E). The T_N of the average valence phase is low and cannot be reached before the transition to the *Am* phase. Measurements on $SrFeO_3$, on the other hand, show a normal second order transition from the *Pa* phase to the antiferromagnetic average valence phase (*Aa*).

For comparison, very characteristic behavior of $CaFeO_3$ is described in brief below (for details, see Refs. (*8*) and (*15*)). Firstly, the monotonically decreasing Hi's of Fe^{3+} and Fe^{5+} can be observed up to the T_N (116 K) and the coexistence of the paramagnetic pattern is, if it occurs, limited to within a few degrees below the T_N. Secondly, in the paramagnetic phase a pair of lines with the same intensities and the same widths are seen over a wide temperature range. The line positions below about 180 K are close to the extrapolated CS's of Fe^{3+} and Fe^{5+}. The separation between the lines decreases gradually above 180 K and more sharply above about 260 K to vanish at about 290 K. One possible explanation is the presence of a quadrupole interaction, and the other is the charge disproportionation proceeding below about 290 K. After having observed the coexistence of the *Pa* and the *Am* phases in some other compositions, we feel it more natural to consider these spectra as indicating the paramagnetic mixed valence phase (*Pm*) which makes a second order antiferromagnetic transition to the *Am* phase. Thus, the electronic transitions in the two contrastive oxides, $CaFeO_3$ and $SrFeO_3$, can be summarized as follows.

$$CaFeO_3: Pa\text{–}(290\ \text{K}) \rightarrow Pm\text{–}(116\ \text{K}) \rightarrow Am,$$

and

$$SrFeO_3: Pa\text{–}(134\ \text{K}) \rightarrow Aa.$$

It is interesting to note here that our unpublished ME measurements revealed that $Ca_{0.5}Sr_{0.5}FeO_3$ behaves similarly to sample (C) in the intermediate temperature range. Thus, partial substitution of Ca^{2+} or La^{3+} for Sr^{2+} in $SrFeO_3$ results in another type of transition. Sample (C) represents this group of oxides, and its behavior can be summarized as follows.

$$Sr_{0.7}La_{0.3}FeO_3: Pa\text{–}(190\text{–}130\ \text{K}) \rightarrow Am.$$

Acknowledgments

The authors are indebted to Professor T. Takada and Professor T. Shinjo for allowing the use of the Mössbauer spectrometers and to Professor M. Shimada for treating samples under high oxygen pressures and also for supplying the $SrFeO_3$ sample. This research was supported financially in part by Grant-in-Aid for Scientific Research from the Ministry of Education, Science, and Culture and also in part by Grants for Fundamental Research in Chemistry from Japan Society for the Promotion of Science.

References

1. J. B. MacChesney, R. C. Sherwood, and J. F. Potter, *J. Chem. Phys.* **43**, 1907 (1965).
2. T. Takeda, Y. Yamaguchi, and H. Watanabe, *J. Phys. Soc. Japan* **33**, 967 (1972).
3. P. K. Gallagher, J. B. MacChesney, and D. N. E. Buchanan, *J. Chem. Phys.* **41**, 2429 (1964).
4. Y. Takeda, S. Naka, M. Takano, T. Shinjo, T. Takada, and M. Shimada, *Mater. Res. Bull.* **13**, 61 (1978).

5. M. TAKANO, N. NAKANISHI, Y. TAKEDA, S. NAKA, AND T. TAKADA, *Mater. Res. Bull.* **12,** 923 (1977).
6. K. A. MÜLLER, TH. VON WALDKIRCH, W. BERLINGER, AND B. W. FAUGHNAN, *Solid State Comm.* **9,** 1097 (1971).
7. Y. TAKEDA, S. NAKA, M. TAKANO, AND N. NAKANISHI, *J. Phys. Colloq.* **40,** C2-331 (1979).
8. M. TAKANO, N. NAKANISHI, Y. TAKEDA, AND S. NAKA, *J. Phys. Colloq.* **40,** C2-313 (1979).
9. M. TAKANO, N. NAKANISHI, Y. TAKEDA, AND T. SHINJO, *in* "Proceedings, 3rd International Conference on Ferrites," in press.
10. U. SHIMONEY AND J. M. KUNDSEN, *Phys. Rev.* **144,** 361 (1966).
11. P. K. GALLAGHER AND J. B. MACCHESNEY, *Symp. Faraday Soc.* **1,** 40 (1968).
12. S. KUME, F. KANAMARU, Y. SHIBASAKI, N. KOIZUMI, K. YASUNAMI, AND T. FUKUDA, *Rev. Sci. Instrum.* **42,** 1856 (1971).
13. M. EIBSCHUTZ, E. HERMON, AND S. SHTRIKMAN, *Phys. Rev.* **156,** 562 (1967).
14. M. TAKANO, N. NAKANISHI, AND T. SHINJO, submitted for publication.
15. T. SHINJO, M. TAKANO, N. HOSOITO, Y. TAKEDA, AND T. TAKADA, *in* "Proceedings, 3rd International Conference on Ferrites," in press.